Electron Accumulation in Nanostructured TiO_2 (Anatase) Electrodes

Gerrit Boschloo and Donald Fitzmaurice*

Department of Chemistry, University College Dublin, Belfield, Dublin 4, Ireland

Received: July 16, 1998; In Final Form: May 13, 1999

If both the technological and commercial potential of nanostructured metal oxide electrodes are to be fully realized, it will be important to understand the effects of electrolyte composition on the extent of electron accumulation and the nature of charge compensation at different applied potentials. Having studied the potential dependent optical absorption spectroscopy of nanostructured TiO_2 (anatase) electrodes in different electrolytes, we concluded that the extent and nature of charge accumulation and compensation depends on whether the potential applied corresponds to weak (<40 mC cm^{-2}) or strong (>40 mC cm^{-2}) accumulation conditions, on whether the electrolyte is prepared using a protic or aprotic solvent, and on whether the ions present in the electrolyte are capable of being intercalated or not.

Introduction

Nanoporous-nanocrystalline metal oxide electrodes have been incorporated in electrochromic windows[1−3] and in ion-insertion batteries.[4] They have also been incorporated, following dye sensitization, in regenerative photoelectrochemical cells.[5,6] It is increasingly clear that nanoporous-nanocrystalline metal oxide electrodes have significant technological and commercial potential.

Nanoporous-nanocrystalline electrodes, referred to as nanostructured electrodes, generally consist of a porous film of interconnected nanocrystals deposited on a conducting support. There are two particularly distinguishing characteristics of nanostructured electrodes: First, the electrolyte penetrates the nanoporous structure of the electrode, and second, the absolute surface area greatly exceeds the geometric surface area. To date, nanostructured electrodes have been prepared from the following metal oxides, which are also wide band gap n-type semiconductors: TiO_2,[1−28] ZnO,[28−33] SnO_2,[28,34−36] Fe_2O_3,[37] WO_3,[38] and Nb_2O_5 and Ta_2O_5.[28]

If the technological and commercial potential of nanostructured metal oxide electrodes are to be fully realized, it will be necessary to understand the effects of nanostructure, surface modification, and electrolyte composition on trap and band state energetics, charge accumulation and compensation, and charge transport and transfer. This paper presents the findings of a study, the principle objective of which was an improved understanding of the effects of electrolyte composition on electron accumulation and compensation in nanostructured TiO_2 (anatase).

Electrochemical techniques are routinely used to understand the effects of electrolyte composition on the extent and nature of electron accumulation and compensation in single crystal metal oxide electrodes.[39,40] These techniques, however, are generally not useful when applied to nanostructured metal oxide electrodes.[12] Consequently, spectroelectrochemical techniques have been developed which take advantage of the facts that thin nanostructured metal oxide films may be deposited on conducting glass supports to yield transparent electrodes and that electrons present in these electrodes have an optical spectroscopy characteristic of their local environment.

The development of these spectroelectrochemical techniques was suggested by experiments reported by Liu and Bard.[41] While measuring the potential dependent optical absorption spectrum of a thin-layer CdS electrode, these workers observed a reversible bleach in the band gap region at negative applied potentials. As band filling gives rise to an apparent increase in the band gap energy, known as a Burstein shift,[42] the observed bleach was assigned to electron accumulation in the conduction band states of the semiconductor electrode.

Fitzmaurice and co-workers adapted this approach to study electron accumulation and compensation in nanostructured TiO_2 (anatase) electrodes.[7−15] In addition to a bleach in the band gap region at negative applied potentials, these workers observed a monotonically increasing absorption extending to the near-infrared. The former, as above, was accounted for by the apparent increase in band gap energy that accompanies band filling.[42] The latter, was assigned to intra- and interband transitions by electrons occupying the conduction band states.[43] An additional spectral feature, namely a pH dependent absorption maximum in the near-infrared, was assigned to electrons localized in surface trap (Ti^{IV}) states.[39]

As pointed out by these workers, the applied potentials at which the spectral changes assigned to the accumulation of electrons in surface trap and conduction band states are observed is related to the energy of the trap and conduction band states being filled. On this basis, a quantitative band filling model was developed that assumed a Schottky junction at the SLI and predicted the existence of an accumulation layer thin enough to follow the contours of the nanostructured electrode at applied potentials more negative than that of the conduction band edge (V_{cb}) at the semiconductor−liquid electrolyte interface (SLI).[9] A fit to experimental data yields values, given by eq 1, for the flatband potential (V_{fb}) of a nanostructured TiO_2 electrode in an aqueous electrolyte.

$$V_{fb}\,(\mathrm{V, SCE}) = -0.40 - (0.06\mathrm{pH}) \qquad (1)$$

Using this approach, Fitzmaurice and co-workers determined V_{fb} for nanostructured TiO_2 electrodes under different conditions.[9−15] In protic solvents, such as water, V_{fb} depended on pH (Nernstian) but not on the nature or concentration of the

* To whom correspondence should be addressed.

10.1021/jp983040m CCC: $18.00 © 1999 American Chemical Society
Published on Web 08/27/1999

electrolyte cation.[7,9] In aprotic solvents, such as acetonitrile (autoprotolysis constant of 3×10^{-27}), V_{fb} depended on both the nature and concentration of the electrolyte cation.[10,13] It was concluded that V_{fb} is determined by the proton adsorption−desorption equilibrium established at the SLI in protic electrolytes. In aprotic electrolytes, however, V_{fb} is determined by the cation adsorption−desorption equilibrium established at the SLI.

It must be pointed out, however, that there has been some controversy concerning the use of a band-filling model to account for the potential dependent optical absorption spectroscopy of nanostructured TiO_2 electrodes and to determine V_{fb}.

It has been proposed that the optical absorption spectroscopy of nanostructured metal oxide electrodes may be fully accounted for by trap filling,[19,31,32] i.e., that there is no band filling. For example, Cao et al. have proposed that electrons accumulated in nanostructured TiO_2 electrodes in protic electrolytes are, having observed surface Ti^{III} states by EPR at 70 K, trapped at surface Ti^{IV} states and compensated by cations in the Helmholtz layers.[19] These workers also suggested that filling of these surface states leads to band edge unpinning.

It has also been proposed that the optical spectroscopy of nanostructured metal oxide electrodes may be fully accounted for by electron trapping on lattice sites accompanied by cation intercalation,[1,16,17,22−27,34] i.e., that there is no band filling. For example, Hagfeldt et al. have proposed that electrons accumulate in nanostructured TiO_2 electrodes in aprotic electrolytes occupy lattice sites and are compensated by intercalated Li^+ ions having observed bulk Ti^{III} sites by XPS.[24−27]

This objective of the study, therefore, was to establish which of the following accounts for the optical absorption spectroscopy of nanostructured TiO_2 (anatase) electrodes in different protic and aprotic electrolytes: the occupation of surface states by electrons charge-compensated by protons or cations in the electrolyte or adsorbed at the SLI, the occupation of conduction band states by electrons charge-compensated by protons or cations in the electrolyte or adsorbed at the SLI, the occupation of lattice sites by electrons charge-compensated by intercalated protons or cations, or a combination of any or all of the above. The paper concludes by considering what general conclusions can be drawn about the relationship between the extent and nature of charge accumulation and compensation in nanostructured metal oxides and electrolyte composition.

Experimental Section

Nanostructured electrodes were prepared, as described in detail elsewhere, by depositing and firing a TiO_2 nanocrystal sol on a conducting glass substrate.[1] Briefly, a colloidal dispersion of TiO_2 nanocrystals was prepared by hydrolysis of titanium isopropoxide (Fluka). This dispersion was stirred at 80 °C for 8 h and autoclaved at 200 °C for 12 h, whereupon the TiO_2 nanocrystals have increased in diameter to 10 nm and consist of pure anatase. The above dispersion was concentrated (16 wt % TiO_2), Carbowax 20000 added (40 wt % of TiO_2), and the resulting sol stirred overnight. The above sol was spread using a glass rod on fluorine-doped tin oxide conducting glass (Glastron, 10 Ω sq^{-1}) masked by Scotch tape. After drying in air, the gel film was fired for 2 h at 450 °C in air. The resulting nanostructured TiO_2 electrode was 4 μm thick and optically transparent.

A nanostructured TiO_2 film supported on conducting glass (geometric surface area 1 cm^2) served as the working electrode in a glass single-compartment three-electrode cell. The counter and reference electrodes were platinum and Ag/AgCl/saturated KCl(aq), respectively. In the case of nonaqueous electrolytes, the reference electrode was connected to the cell via a salt bridge. The electrolyte was thoroughly deaerated by bubbling with Ar or N_2. All potentials are reported against Ag/AgCl/saturated KCl(aq). The above cell was incorporated in the sample compartment of a Hewlett-Packard 8452A diode array spectrophotometer and connected to a Solartron SI 1287 potentiostat. All cyclic voltammograms (CVs) were recorded, following a number of initial conditioning CVs, at a scan rate of 10 mV s^{-1}. All optical absorption spectra were measured against a background recorded at 0.00 V.

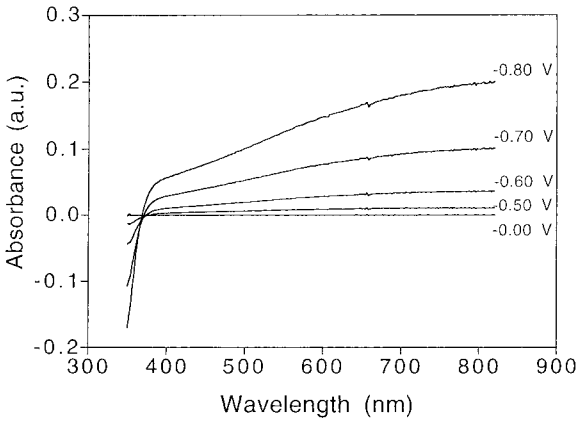

Figure 1. Optical absorption spectra of a nanostructured TiO_2 electrode measured at pH 2.0 in an aqueous electrolyte ($LiClO_4$, 0.2 mol dm^{-3}) following polarization for 60 s at the indicated applied potential.

$LiClO_4$, $NaClO_4$, tetramethylammonium perchlorate ((TMA)ClO_4), and tetrabutylammonium perchlorate ((TBA)ClO_4) were purchased from Aldrich and dried under reduced pressure at 150 °C for 48 h prior to use. $LiOH{\cdot}H_2O$ and tetramethylammonium hydroxide ((TMA)OH, 25 wt % solution in water) were also purchased from Aldrich. Acetonitrile was refluxed over P_2O_5 for 3 h and the middle fraction used immediately following recovery or stored over activated molecular sieves.

Results

Aqueous Electrolytes. Shown in Figure 1 are the potential dependent optical absorption spectra of a nanostructured TiO_2 electrode measured in an aqueous electrolyte containing Li^+ ions ($LiClO_4$, 0.2 mol dm^{-3}) at pH 2.0. Application of a sufficiently negative potential results in an absorbance decrease and increase at wavelengths shorter and longer, respectively, than the onset for band gap excitation (380 nm). It is noted that potential dependent spectra measured at pH 12.0 are similar to those measured at pH 2.0 but shifted to more negative potentials by 0.6 V (not shown). It is noted also that potential dependent spectra similar to those measured in an electrolyte containing Li^+ ions are measured in an electrolyte containing Na^+ ($NaClO_4$, 0.2 mol dm^{-3}) or TMA^+ ions (V_{fb4}, 0.1 mol dm^{-3}) at either pH 2.0 or pH 12.0 (not shown).

Shown in Figure 2a are CVs of a nanostructured TiO_2 electrode measured in an aqueous electrolyte containing Li^+ ions ($LiClO_4$, 0.2 mol dm^{-3}) at pH 2.0 and 12.0. Shown in Figure 2b are the absorbance changes measured simultaneously at 350 and 700 nm. It is noted that the current and absorbance changes measured at pH 12.0 are similar to those measured at pH 2.0 but shifted to more negative potentials by 0.6 V. It is noted also that similar current and absorbance changes are measured in an electrolyte containing Na^+ ($NaClO_4$, 0.2 mol dm^{-3}) or TMA^+ ions (V_{fb4}, 0.1 mol dm^{-3}) at either pH 2.0 or 12.0 (not shown).

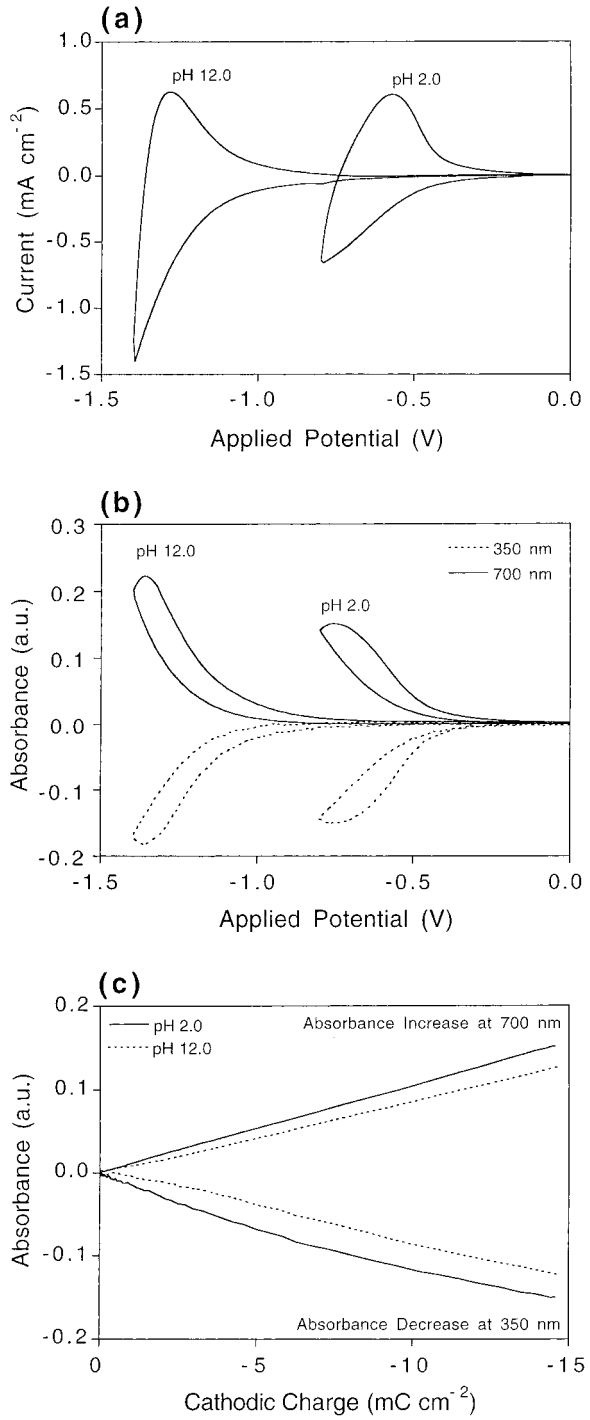

Figure 2. (a) Cyclic voltammograms of a nanostructured TiO_2 electrode measured at pH 2.0 and pH 12.0 in an aqueous electrolyte ($LiClO_4$, 0.2 mol dm^{-3}). (b) Absorbance changes measured at 350 and 700 nm while recording cyclic voltammograms in (a). (c) Absorbance decrease at 350 nm and absorbance increase at 700 nm in (b) versus cathodic charge calculated from CVs in (a).

Numerical integration of the CVs in Figure 2a, yields values for the anodic (dis)charge and cathodic charge. It is noted that values as high as 0.93 have been obtained for the ratio of the anodic discharge to the cathodic charge (CR). Lower CR values are obtained if residual oxygen is present, if the applied potential is scanned to values that are 0.3 V more negative than V_{fb} due to hydrogen evolution, or if the scan rate is increased. It is noted also, that similar CRs are measured in an electrolyte containing Na^+ ($NaClO_4$, 0.2 mol dm^{-3}) or TMA^+ ions (V_{fb4}, 0.1 mol dm^{-3}) at either pH 2.0 or 12.0.

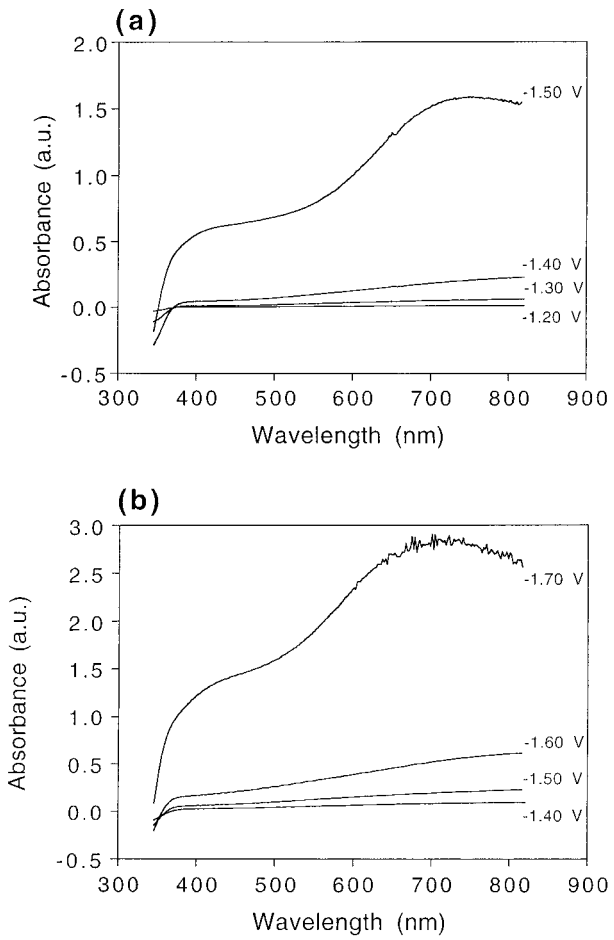

Figure 3. (a) Optical absorption spectra of a nanostructured TiO_2 electrode measured in a strongly basic (~pH 14.0) aqueous electrolyte (LiOH, 1.0 mol dm^{-3}) following polarization for 60 s at the indicated applied potential. (b) As in (a) for (V_{fb}, 1.0 mol dm^{-3}).

Plotting the cathodic charge (Figure 2a) against the corresponding absorbance increase and decrease at 700 and 350 nm, respectively (Figure 2b), yields, as may be seen in Figure 2c, a linear relationship for a nanostructured TiO_2 electrode in an aqueous electrolyte containing Li^+ ions ($LiClO_4$, 0.2 mol dm^{-3}) at either pH 2.0 or 12.0. A linear relationship is also observed when the anodic discharge is plotted against the corresponding absorbance decrease and increase at 700 and 350 nm, respectively. Similar relationships are obtained in an electrolyte containing Na^+ ($NaClO_4$, 0.2 mol dm^{-3}) or TMA^+ ions (V_{fb4}, 0.1 mol dm^{-3}) at either pH 2.0 or 12.0.

According to eq 2, where $\Delta A(\lambda)$ is the change in absorbance at a wavelength λ and ΔQ is the cathodic charge or anodic discharge responsible for the absorbance change, the slopes of the plots in Figure 2c yield values for the coloration efficiency (CE).

$$CE(\lambda) = \Delta A(\lambda)/\Delta Q \qquad (2)$$

A coloration efficiency of 9 cm^2 C^{-1} at 700 nm is measured during cathodic charging for aqueous electrolytes containing Li^+, Na^+, or TMA^+ ions at either pH 2.0 or 12.0. If it is assumed that the leakage current is small, this implies an average extinction coefficient of 900 mol^{-1} dm^3 cm^{-1} at 700 nm for the electrons present in the nanostructured TiO_2 electrode.

Strongly Basic Aqueous Electrolytes. Shown in Figure 3 are the potential dependent optical absorption spectra of a nanostructured TiO_2 electrode measured in a strongly basic

aqueous electrolyte containing Li^+ (LiOH, 1.0 mol dm^{-3}) or TMA^+ ions (V_{fb}, 1.0 mol dm^{-3}) at approximately pH 14.0. At negative applied potentials, the spectra measured in an electrolyte containing Li^+ or TMA^+ ions are in excellent agreement and, in both cases, qualitatively similar to those shown in Figure 1. At more negative applied potentials, however, the spectra measured in an electrolyte containing Li^+ ions increase in intensity relative to those measured in an electrolyte containing TMA^+ ions and exhibit a pronounced maximum at 750 nm. At still more negative potentials, a maximum is also observed in an electrolyte containing TMA^+ ions. The potential dependent spectra (not shown) measured for a nanostructured TiO_2 electrode in a strongly basic aqueous electrolyte containing Na^+ ions (NaOH, 1.0 mol dm^{-3}) at approximately pH 14.0 are qualitatively similar to those measured under the same conditions in an electrolyte containing TMA^+ ions (not shown).

Shown in Figure 4a are CVs of a nanostructured TiO_2 electrode measured in a strongly basic aqueous electrolyte containing Li^+ (LiOH, 1.0 mol dm^{-3}), Na^+ (NaOH, 1.0 mol dm^{-3}), or TMA^+ ions (V_{fb}, 1.0 mol dm^{-3}) at approximately pH 14.0. It is noted that compared to an electrolyte containing Li^+ ions, the onset for accumulation is shifted to more negative potentials by about 0.1 V in an electrolyte containing Na^+ or TMA^+ ions. It is noted also that a more pronounced anodic peak is observed in an electrolyte containing Li^+ ions and that this peak is shifted to significantly more positive potentials than in an electrolyte containing Na^+ or TMA^+ ions. The CRs (from Figure 4a) in an electrolyte containing Li^+, Na^+, or TMA^+ ions are 0.72, 0.68, and 0.67, respectively. These values decrease significantly, however, as the scan rate is increased.

Shown in Figure 4b are the absorbance increases (and decreases during the reverse sweep) measured simultaneously at 700 nm. It is noted that compared to an electrolyte containing Li^+ ions, the absorbance onset is observed at more negative potentials by about 0.1 V in an electrolyte containing Na^+ or TMA^+ ions. It is noted also that, compared to an electrolyte containing Li^+ ions, the observed hysteresis is smaller in an electrolyte containing Na^+ or TMA^+ ions.

Plotting the cathodic charge (Figure 4a) against the corresponding absorbance increase at 700 nm (Figure 4b) yields, as may be seen in Figure 4c, a nonlinear relationship for a nanostructured TiO_2 electrode in a strongly basic aqueous electrolyte containing Li^+ ions (LiOH, 1.0 mol dm^{-3}) at approximately pH 14.0. Specifically, a pronounced change in the slope is observed following accumulation of 40 mC cm^{-2} of charge. No significant change in slope, however, is observed under the same conditions in a strongly basic electrolyte containing Na^+ (NaOH, 1.0 mol dm^{-3}) or TMA^+ ions ((TMA)-OH, 1.0 mol dm^{-3}). In an electrolyte containing Li^+ ions, therefore, the coloration efficiency increases from an initial value of 10 cm^2 C^{-1} to a final value of 26 cm^2 C^{-1} at 700 nm. In an electrolyte containing Na^+ or TMA^+ ions, however, the coloration efficiency remains constant and lies in the range 9−10 cm^2 C^{-1} at 700 nm. If it is assumed that the leakage current from the nanostructured TiO_2 electrode is small, then in an electrolyte containing Li^+ ions the average extinction coefficient at 700 nm for an electron accumulated in nanostructured TiO_2 increases from an initial value of 1000 mol^{-1} dm^3 cm^{-1} to a final value of 2600 mol^{-1} dm^3 cm^{-1}. In an electrolyte containing Na^+ or TMA^+ ions, however, the average extinction coefficient at 700 nm remains constant and lies in the range 900−1000 mol^{-1} dm^3 cm^{-1}.

Acetonitrilic Electrolytes. Shown in Figure 5 are the potential dependent optical absorption spectra of a nanostructured TiO_2 electrode measured at the indicated applied potentials in an acetonitrilic electrolyte containing Li^+ ions ($LiClO_4$, 1.0 mol dm^{-3}). At moderately negative applied potentials the measured spectra are similar to those shown in Figures 1 and 3. At still more negative applied potentials a broad absorption maximum, similar to that in Figure 3, is observed at about 750 nm. It is noted that the spectra measured for a nanostructured TiO_2 electrode in an acetonitrilic electrolyte containing Na^+ ions ($NaClO_4$, 1.0 mol dm^{-3}) are qualitatively similar, although more negative potentials must be applied in order that a given

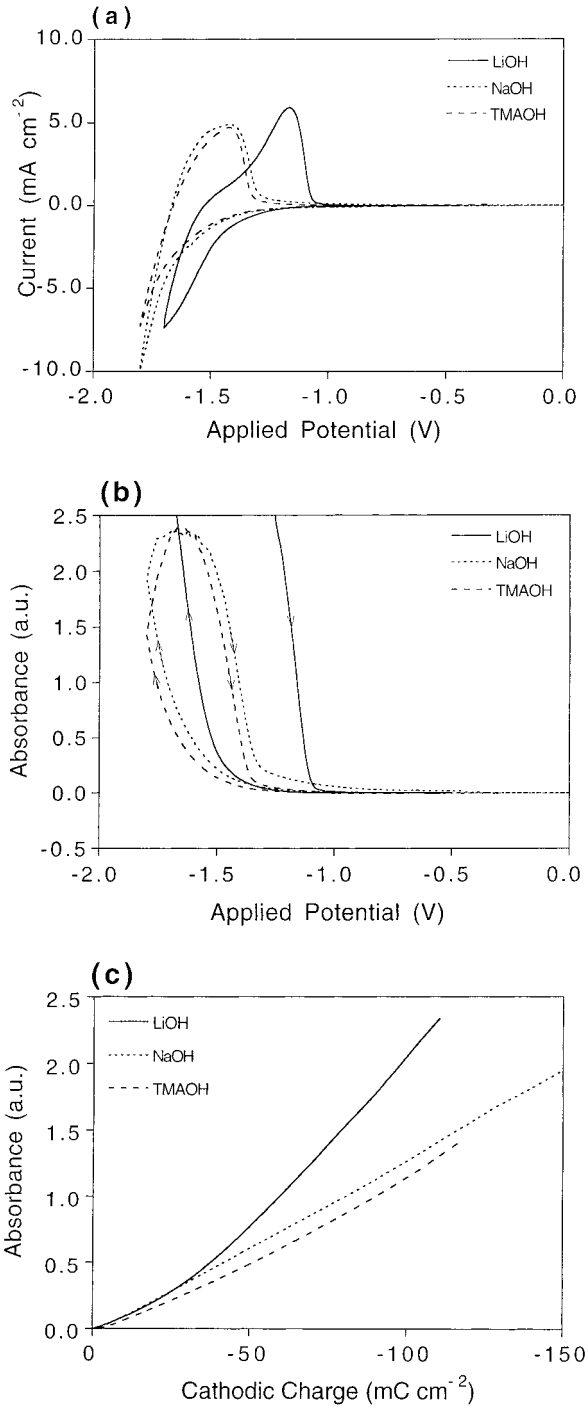

Figure 4. (a) Cyclic voltammograms of a nanostructured TiO_2 electrode measured in a strongly basic (∼pH 14.0) aqueous electrolyte (LiOH, NaOH or V_{fb}, 1.0 mol dm^{-3}). (b) Absorbance changes measured 700 nm while recording cyclic voltammograms in (a). (c) Absorbance increase at 700 nm in (b) versus cathodic charge calculated from CVs in (a).

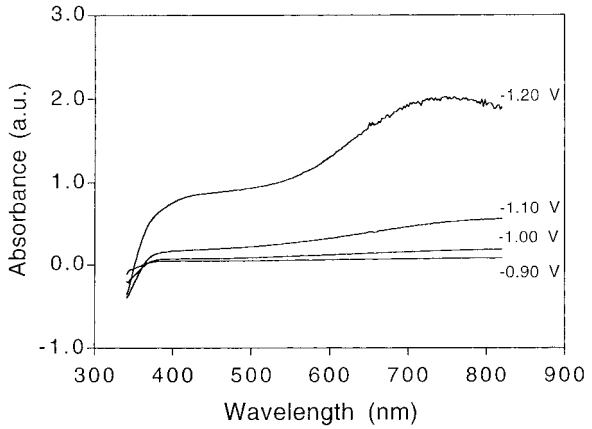

Figure 5. Optical absorption spectra of a nanostructured TiO_2 electrode measured in dry acetonitrilic electrolyte ($LiClO_4$, 1.0 mol dm^{-3}) following polarization for 60 s at the indicated applied potential.

absorbance change be observed (not shown). It is noted that the spectra measured for nanostructured TiO_2 electrode in acetonitrilic electrolyte containing TBA^+ ions (V_{fb4}, 0.2 mol dm^{-3}) are qualitatively similar, although no absorption maximum is detected at any measured applied potential and even more negative potentials must be applied in order to observe a given absorbance change (not shown).

Shown in Figure 6a are the CVs of a nanostructured TiO_2 electrode measured in an acetonitrilic electrolyte containing Li^+ ($LiClO_4$, 1.0 mol dm^{-3}), Na^+ ($NaClO_4$, 1.0 mol dm^{-3}), or TBA^+ ions (V_{fb4}, 0.2 mol dm^{-3}). The CRs for electrolytes containing Li^+ and Na^+ ions are 0.95 and 0.80, respectively. The CR for an electrolyte containing TBA^+ ions, however, was zero, indicating irreversible electrochemical side reactions. Concerning the dependence CR on scan rate, we note the following: The CR is generally greater than 0.7 for scan rates of 10 mV s^{-1} but decreases significantly as the scan rate is increased due to competing side reactions.

Shown in Figure 6b are the absorbance increases measured simultaneously at 700 nm. It is noted that compared to an electrolyte containing Li^+ ions the absorbance onset is observed at more negative potentials by about 0.5 and 1.0 V in an electrolyte containing Na^+ or TBA^+ ions, respectively. It is also noted that in the case of an electrolyte containing TBA^+ ions the current and absorption onset occurred at significantly more positive potentials following prolonged stabilization (30 min) in the electrolyte, presumably due to slow adsorption of trace water molecules at the TiO_2 surface. Under the same conditions it is observed that the CR decreases to about 0.60.

Plotting the cathodic charge (Figure 6a) against the corresponding absorbance increase at 700 nm (Figure 6b) yields, as may be seen in Figure 6c, a nonlinear relationship for a nanostructured TiO_2 electrode in an acetonitrilic electrolyte containing Li^+ ($LiClO_4$, 1.0 mol dm^{-3}) or Na^+ ions ($NaClO_4$, 1.0 mol dm^{-3}). In the case of an acetonitrilic electrolyte containing TBA^+ ions (V_{fb4}, 0.2 mol dm^{-3}) a linear relationship is observed. Specifically, for an electrolyte containing Li^+ or Na^+ ions a pronounced change in the slope is observed after accumulation of 40 mC cm^{-2} of charge. The initial slope is the same in both cases and yields values for the coloration efficiency that lie in the range 7−9 cm^2 C^{-1} at 700 nm. The final slope is not the same and yields values for the coloration efficiency of 29 and 23 cm^2 C^{-1} at 700 nm, respectively. If it is assumed that the leakage current from the nanostructured TiO_2 electrode is small, then the average extinction coefficient at 700 nm for an electron accumulated in nanostructured TiO_2 increases from

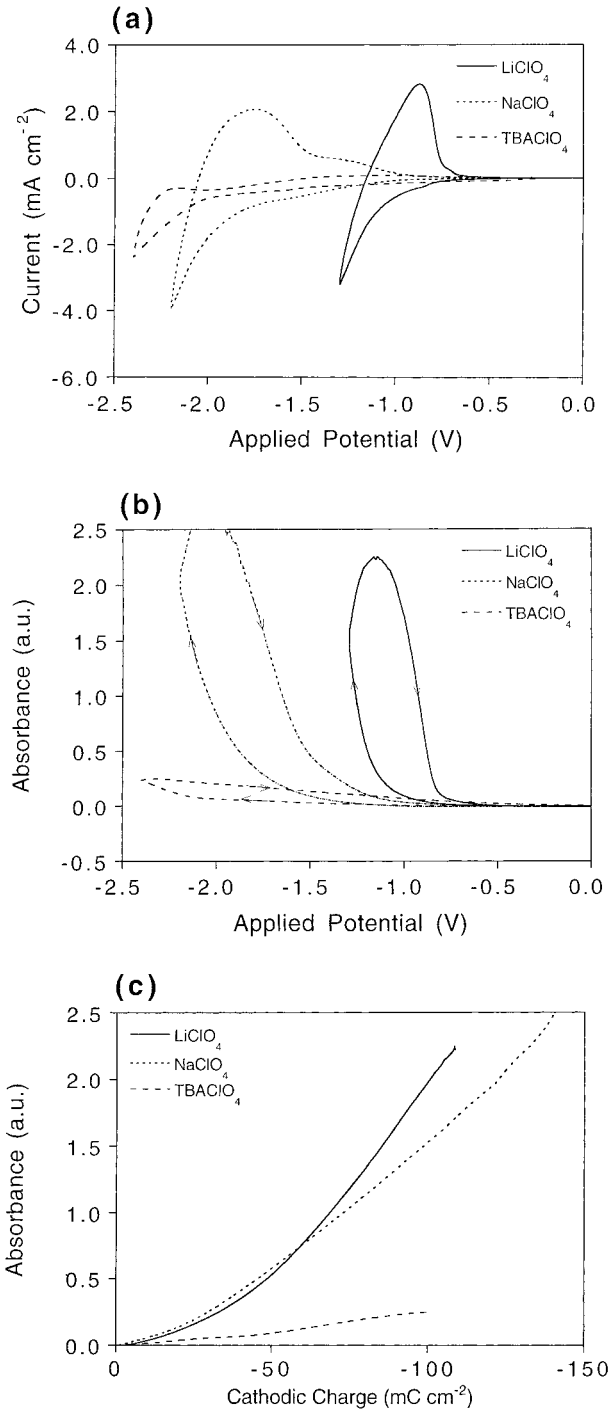

Figure 6. (a) Cyclic voltammograms of a nanostructured TiO_2 electrode measured in a dry acetonitrilic electrolyte ($LiClO_4$, $NaClO_4$, 1.0 mol dm^{-3} or $(TBA)ClO_4$, 0.2 mol dm^{-3}). (b) Absorbance changes measured 700 nm while recording cyclic voltammograms in (a). (c) Absorbance increase at 700 nm in (b) versus cathodic charge calculated from CVs in (a).

an initial value that lies in the range 700−900 mol^{-1} dm^3 cm^{-1} for an electrolyte containing Li^+ and Na^+ ions to final values of 2800 and 2200 mol^{-1} dm^3 cm^{-1}, respectively. In the case of an electrolyte containing TBA^+ ions, the coloration efficiency (4 cm^2 C^{-1} at 700 nm), although lower, is constant over the potential range studied (up to 100 mC cm^{-2}).

Discussion

As stated, if both the technological and commercial potential of nanostructured metal oxide electrodes are to be fully realized,

it will be important to understand the effects of electrolyte composition on the extent and nature of electron accumulation and compensation at different applied potentials.

Having studied the potential dependent optical absorption spectroscopy of nanostructured TiO_2 (anatase) electrodes in different electrolytes, we concluded that the extent of accumulation and the nature of charge compensation depends on whether the potential applied corresponds to weak (<40 mC cm^{-2}) or strong (>40 mC cm^{-2}) accumulation conditions, on whether the electrolyte is prepared using a protic or aprotic solvent, and on whether the ions present in the electrolyte are capable of being intercalated or not. The discussion that follows presents the evidence supporting these conclusions.

Weak Accumulation-Band-Filling. The potential dependent optical absorption spectra of nanostructured TiO_2 (Figures 1, 3, and 5) is characterized, under weak accumulation conditions, by an absorbance decrease at wavelengths shorter than that corresponding to the onset of band gap excitation (380 nm). This absorbance decrease is assigned to the Burstein shift that accompanies filling of conduction band states by accumulated electrons.[42] At longer wavelengths these spectra are characterized by a monotonically increasing absorbance.[43] This absorbance increase is assigned to intra- and interband transitions by electrons accumulated in conduction band states and is readily accounted for by Drude theory modified to take into account scattering by phonons or ionized impurities. It is noted that a weak absorption band is observed at about 900 nm in experiments performed over an extended wavelength range.[7,9] Principally as a consequence of the pH dependence of this band, it has been assigned to electrons localized in surface states.[7,9]

Having studied the potential dependence of these spectra under weak accumulation conditions in different aqueous (Figure 1), strongly basic (Figure 3) and acetonitrilic (Figure 5) electrolytes, one may make a number of observations.

In the case of nanostructured TiO_2 in an aqueous electrolyte these include the following: First, the onset potential for charge accumulation (Figure 2a) and for both the Burstein shift and the Drude absorption (Figure 2b) are the same and show the expected Nernstian shift (0.6 V) on increasing the pH of the electrolyte from 2.0 to 12.0. Second, the onset potentials for charge accumulation (Figure 2a) and for both the Burstein shift and the Drude absorption (Figure 2b) are not dependent on the electrolyte. Third, the coloration efficiency (9 cm^2 C^{-1}) and average extinction coefficient (900 mol^{-1} dm^3 cm^{-1}) are constant and independent of electrolyte composition (Figure 2c).

In the case of nanostructured TiO_2 in a strongly basic aqueous electrolyte these include the following: First, the onset for charge accumulation (Figure 4a) shows the expected Nernstian shift (0.7 V) on increasing the pH of the electrolyte from 2.0 (Figure 2a) to approximately 14.0. Second, the onset for charge accumulation (Figure 4a) and the onset potential for Drude absorption (Figure 4b) are dependent on the electrolyte. Specifically, both are observed at more positive potentials in electrolytes containing Li^+ ions than in electrolytes containing Na^+ or TMA^+ ions. Third, the coloration efficiencies (9$-$10 cm^2 C^{-1}) and average extinction coefficients (900$-$1000 mol^{-1} dm^3 cm^{-1}) are constant and independent of the electrolyte (Figure 4c).

In the case of nanostructured TiO_2 in an acetonitrilic electrolyte these include the following: First, the onset for charge accumulation (Figure 6a) shows the expected Nernstian shift to more negative potentials in an aprotic electrolyte (autoprotolysis constant 3×10^{-27}). Second, the onset for charge accumulation (Figure 6a) and the onset potential for the Drude absorption (Figure 6b) are dependent on the electrolyte. Specifically, both are observed at increasingly more negative potentials in electrolytes containing Li^+, Na^+, and TBA^+ ions, respectively. Third, the coloration efficiency (about 7 cm^2 C^{-1}) and average extinction coefficient (about 700 mol^{-1} dm^3 cm^{-1}) are similar for electrolytes containing Li^+ and Na^+ ions but significantly less for electrolytes containing TBA^+ ions (4 cm^2 C^{-1}) due to side reactions.

To account for the observed potential dependence of the optical absorption spectroscopy of nanostructured TiO_2 on electrolyte composition under weak accumulation conditions, the following model is proposed.

As the surface of nanostructured TiO_2 is hydroxylated, the two equilibria represented by eqs 3 and 4 determine the surface charge in protic electrolytes.[39]

$$Ti^{IV}{}_s{-}OH + H^+ \rightleftharpoons Ti^{IV}{}_s{-}OH_2{}^+ \quad (3)$$

$$O^-{}_s + H^+ \rightleftharpoons O_sH \quad (4)$$

In aprotic electrolytes, however, where M^+ denotes the electrolyte cation, it is the two equilibria represented by eqs 5 and 6 that determine the surface charge.[10,39]

$$Ti^{IV}{}_s{-}OH + M^+ \rightleftharpoons Ti^{IV}{}_s{-}OHM^+ \quad (5)$$

$$O^-{}_s + M^+ \rightleftharpoons O_sM \quad (6)$$

That is, the surface charge is determined by proton adsorption/desorption in protic electrolytes[39] and by cation adsorption/desorption in aprotic electrolytes.[10,13] Furthermore, as V_{fb} depends on the surface charge, these equilibria also determine the onset potential for charge accumulation and associated spectroscopic changes in nanostructured TiO_2.

At applied potentials close to V_{fb}, electron accumulation is accompanied by trap filling according to eq 7. That is, electrons occupy surface Ti^{IV} states with the

$$Ti^{IV}{}_s{-}OH + e^- + (M^+ \text{ or } H^+) \rightarrow Ti^{III}{}_s{-}OH(M^+ \text{ or } H^+)_{ads} \quad (7)$$

$$TiO_2 + e^- + (M^+ \text{ or } H^+) \rightarrow TiO_2(e_{cb})(M^+ \text{ or } H^+)_{ads} \quad (8)$$

accumulated charge being compensated by adsorption of a proton or cation from the electrolyte. At applied potentials negative of V_{fb}, however, electron accumulation is accompanied by band filling according to eq 8. That is, electrons occupy conduction band states with the accumulated charge being compensated by adsorption of a proton or a cation from the electrolyte.

Implicit in the above model is the absence of a significant change in the composition of the Helmholtz layer and, consequently, the absence of any significant drop in the applied potential across this layer. In support of this view, an unrealistically large band edge shift of 1.0 V is predicted if it is assumed that a charge of 40 mC cm^{-2} (50 μC cm^{-2} when corrected for surface roughness) is accumulated in the Helmholtz layer (50 μF cm^{-2} corrected for surface roughness),[44] which is the case when no adsorption takes place.

A question that arises is the relative contribution of trap (eq 7) and conduction band state filling (eq 8) to the measured spectroscopic changes and, therefore, also to electron accumulation.

As mentioned in the Introduction, it has been suggested that the potential dependent optical absorption spectroscopy of

nanostructured TiO_2 in protic electrolytes may be fully accounted for by electron trapping in surface Ti^{IV} states and charge compensation by protons or cations in the Helmholtz layer.[19] If, however, this were the case, it would not be expected that the absorbance increase measured at 700 nm and the absorbance decrease measured at 350 nm would be correlated. Furthermore, it would not be expected that the absorbance observed at longer wavelengths would increase monotonically. Rather, it would be expected that the measured absorption spectra would show a pronounced pH dependent absorption maximum.[7,9,45] In short, there is no spectral evidence for trapping of electrons in nanostructured TiO_2 under weak accumulation conditions.

A possible explanation for this observation is that the number of surface Ti^{IV} state traps is such that their occupation by accumulated electrons is not detected spectroscopically. In support of this view it is noted that less than 4% of surface Ti^{IV} atoms states, about 2×10^{13} cm^{-2}, act as traps; the remainder lie inside the conduction band.[40,46,47] For a nanostructured TiO_2 electrode that is 4 μm thick and has a porosity of 50%, a specific surface area of 107 m^2 g^{-1}, and an absolute surface area of 800 cm^2, less than 3 mC cm^{-2} of accumulated charge is required to reduce all available trap states.[23] Clearly, even under weak accumulation conditions ($<$40 mC cm^{-2}) all available trap states are filled and band filling dominates. It should be noted, however, that the preparative history of a nanostructured TiO_2 electrode may be such that the number of surface Ti^{IV} state traps is sufficient to contribute measurably to potential dependent spectroscopy and, possibly, to lead to band edge unpinning.[19]

As also mentioned in the Introduction, it has been suggested that the potential dependent optical absorption spectroscopy of nanostructured TiO_2 may be accounted for by electron accumulation at lattice sites compensated by either proton or cation intercalation.[3,16,17,22−26,34,48] As reported above, the spectra measured under weak accumulation conditions for both protic (water at pH 2.0 and pH 12.0) and aprotic (acetonitrile) electrolytes are in excellent qualitative agreement. Also as reported above, the spectra measured for electrolytes containing cations which do (Li^+ or Na^+ [3,16,22−26,48]) and which do not (TMA^+ or TBA^+ [16,17,34]) intercalate are in excellent qualitative agreement. On this basis it is concluded that if intercalation occurs in protic or aprotic electrolytes, it is only under strong accumulation conditions.

In summary, neither a trap-filling or intercalation model can account for the potential dependent optical absorption spectroscopy of nanostructured TiO_2 under weak accumulation conditions ($<$40 mC cm^{-2}). In fact, and as originally proposed,[7−15] a model that incorporates both trap and conduction band state filling, with the latter dominating, is most appropriate under weak accumulation conditions.

Strong Accumulation−Intercalation. At negative applied potentials, the optical absorption spectra of nanostructured TiO_2 (Figures 1, 3, and 5) are characterized, under strong accumulation conditions ($>$40 mC cm^{-2}), by an absorbance decrease at wavelengths shorter than that corresponding to the onset of band gap absorption (380 nm) and by an absorbance increase at longer wavelengths. At still more negative potentials in aprotic solvents, that is under very strong accumulation conditions, the initially observed decrease in absorbance is partially reversed, while a pronounced absorption maximum develops at about 750 nm.

Having studied the potential dependence of these spectra under strong accumulation conditions in different aqueous (Figure 2), strongly basic (Figure 4), and acetonitrilic (Figure 6) electrolytes, one can make a number of observations.

In the case of nanostructured TiO_2 in an aqueous electrolyte these include the following: First, the potential dependent optical absorption spectra are in excellent qualitative agreement with those measured under weak accumulation conditions (Figure 1). Second, the coloration efficiency (9 cm^2 C^{-1}) and average extinction coefficient (900 mol^{-1} dm^3 cm^{-1}) are the same as those measured under weak accumulation conditions (Figure 2). On this basis, and assuming all surface states are filled, the observed absorbance changes are assigned to filling of conduction band states. Furthermore, the fact that the coloration efficiency and average extinction coefficient remain constant suggest that cation intercalation is not important. In fact, it is possible that cation intercalation occurs at only applied potentials significantly more negative than that of the conduction band edge and that in an aqueous electrolyte, proton intercalation and/or water decomposition compete.[39] It is noted also that, while intercalation of Li^+ or Na^+ ions into TiO_2 (anatase) is well documented,[48] such behavior has only been observed at negative applied potentials in aprotic electrolytes (see below). Clearly, intercalation of TMA^+ ions is sterically forbidden.

In the case of nanostructured TiO_2 in a strongly basic aqueous electrolyte these include the following: First, the potential dependent optical absorption spectra measured in an electrolyte containing Li^+ ions are qualitatively different from those measured under weak accumulation conditions, while the spectra measured in electrolytes containing either Na^+ or TMA^+ ions are qualitatively similar to those measured under weak accumulation conditions. Specifically, in an electrolyte containing Li^+ ions the spectra measured at applied potentials more negative than −1.40 V (Figure 3a) show a pronounced absorption maximum at about 750 nm. By comparison, the spectra measured in electrolytes containing Na^+ or TMA^+ ions do not. Second, there is a marked increase in coloration efficiency (26 cm^2 C^{-1}) and average extinction coefficient (2600 mol^{-1} dm^3 cm^{-1}) following accumulation of about 40 mC cm^{-2} in electrolytes containing Li^+ ions (Figure 4c). By comparison, the coloration efficiency and the average extinction coefficient at 700 nm show no similar increase in an electrolyte containing either Na^+ or TMA^+ ions. On this basis, it is concluded that the mechanism for electron accumulation changes from band filling (eq 8), compensated by adsorption of Li^+ ions, to lattice site filling, compensated by Li^+ ion intercalation, eq 9.

$$TiO_2 + xLi^+ + xe^- \rightarrow Li_xTiO_2(Li_xTi^{III}{}_xTi^{IV}{}_{1-x}O_2) \quad (9)$$

On this basis, it is also concluded that there is no change in the mechanism for electron accumulation in an electrolyte containing either Na^+ or TMA^+ ions.

In the case of nanostructured TiO_2 in an aprotic electrolyte it is possible to conclude the following: First, the potential dependent optical absorption spectra measured in an electrolyte containing either Li^+ or Na^+ ions under strong accumulation conditions are qualitatively different from those measured under weak accumulation conditions, but the spectra measured under both strong and weak accumulation conditions in an electrolyte containing TBA^+ ions are qualitatively similar. Specifically, in an electrolyte containing either Li^+ or Na^+ ions the spectra measured at applied potentials more negative than −1.20 V (Figure 3) and −2.0 V, respectively, or following accumulation of about 40 mC cm^{-2} of charge, show a pronounced absorption maximum at about 750 nm. By comparison, the spectra measured in an electrolyte containing TBA^+ ions do not. Second, there is a marked increase in coloration efficiency (29 and 23 cm^2 C^{-1}, respectively) and average extinction coefficient (2800 and 2200 mol^{-1} dm^3 cm^{-1}, respectively) following

accumulation of about 40 mC cm^{-2} in electrolytes containing Li^+ or Na^+ ions (Figure 4c). By comparison, the coloration efficiency and average extinction coefficient at 700 nm show no similar increase in an electrolyte containing TBA^+ ions. On this basis, it is concluded that there is a change in the mechanism for electron accumulation from band filling (eq 8), compensated by adsorption of either Li^+ or Na^+ ions, to lattice site filling, compensated by either Li^+ or Na^+ ion intercalation (eq 9). Clearly, there is no change in the accumulation mechanism in an electrolyte containing TBA^+ ions, presumably because intercalation is sterically forbidden.

It was noted above that Li^+ ion but not Na^+ ion intercalation is observed in strongly basic electrolytes, while both Li^+ and Na^+ ion intercalation is observed in an aprotic electrolyte. It is suggested, therefore, that in a strongly basic electrolyte proton intercalation and/or water decomposition dominates at applied potentials sufficiently negative to promote Na^+ ion intercalation. In an aprotic electrolyte, however, a sufficient overpotential can be generated to promote Na^+ ion intercalation. In short, the difference in behavior observed for Li^+ and Na^+ relates to the extent of band filling necessary to generate a sufficient overpotential to intercalate a Li^+ or Na^+ ion. It should be noted that this difference in behavior does not relate to the activation energy for the hopping step that accompanies diffusion of either Li^+ or Na^+ ions in nanostructured TiO_2, as this has been determined to be 0.5 eV for both ions.[49]

To account for the observed potential dependence of the optical absorption spectroscopy of nanostructured TiO_2 on electrolyte composition under strong accumulation conditions, the following model is proposed.

In an aqueous electrolyte the surface charge and therefore V_{fb} is determined by the proton adsorption/desorption equilibrium established at the SLI. Under strong accumulation conditions, electrons occupy the available conduction band states and are compensated by adsorbed protons or cations. However, before the extent of band filling is such that there exists a sufficient overpotential to intercalate either Li^+ or Na^+ ions, proton intercalation and/or water decomposition dominates. Clearly, TMA^+ ion intercalation is sterically forbidden.

In a strongly basic aqueous electrolyte the surface charge and therefore V_{fb} is determined principally by the cation adsorption/desorption equilibria established at the SLI (eqs 5 and 6). Under strong accumulation conditions, electrons are accumulated in the available states of the conduction band and are compensated by adsorbed cations. Once this overpotential is sufficient, Li^+ ions are intercalated. However, before the extent of band filling is such that there exists a sufficient overpotential to intercalate Na^+ ions, protons intercalation and/or water decomposition dominate. Clearly TMA^+ ion intercalation is sterically forbidden.

In an aprotic electrolyte, the surface charge and therefore V_{fb} is determined by the cation adsorption/desorption equilibrium established at the SLI. At applied potentials significantly more negative than V_{fb}, that is under strong accumulation conditions, electrons are accumulated in the available states of the conduction band and are compensated by adsorbed cations. Once the extent of band filling is such that there exists a sufficient overpotential for intercalation, ions are inserted into the TiO_2 (anatase) crystal lattice. Thus, both Li^+ or Na^+ ion intercalation is observed although, for steric reasons, TBA^+ ion intercalation is not.

Accumulation-Compensation Kinetics. The reported electrochemical and spectroelectrochemical data do not show, on the time scale on which measurements were made, any evolution. Nevertheless, it must be recognized that intercalation may take place very slowly under certain conditions, for example, under weak accumulation conditions in aprotic solvents. Furthermore, processes occurring on the time scale of days, months, and years may have a significant impact on the performance and stability of devices based on nanostructured metal oxide electrodes.

Conclusions

The potential dependent optical absorption spectroscopy of nanostructured TiO_2 (anatase) electrodes in different electrolytes is explained by a model that takes into account whether the potential applied corresponds to weak (<40 mC cm^{-2}) or strong (>40 mC cm^{-2}) accumulation conditions, whether the electrolyte is prepared using a protic or aprotic solvent, and whether the ions present in the electrolyte are capable of being intercalated or not. Furthermore, this model reconciles previously reported spectroelectrochemical findings for nanostructured TiO_2 (anatase) electrodes and provides important insights into their optimization for a growing number of applications.

Acknowledgment. This work has been supported by the Commission of the European Union under the Joule III program (JOR3-CT96-0107).

References and Notes

(1) Hagfeldt, A.; Vlachopoulos, N.; Grätzel, M. *J. Electrochem. Soc.* **1994**, *141*, L82.
(2) Marguerettaz, X.; O'Neill, R.; Fitzmaurice, D. *J. Am. Chem. Soc.* **1994**, *116*, 2629.
(3) Cinnsealach, R.; Boschloo, G.; Rao, S. N.; Fitzmaurice, D. *Sol. Energy Mater. Sol. Cells* **1999**, *55*, 215.
(4) Huang, S. H.; Kavan, L.; Exnar, I.; Grätzel, M. *J. Electrochem. Soc.* **1995**, *142*, L182.
(5) O'Regan, B.; Grätzel, M. *Nature* **1991**, *353*, 737.
(6) Nazeeruddin, M. K.; Kay, A.; Rodico, I.; Humphry-Baker, R.; Müller, E.; Liska, P.; Vlachopoulos, N.; Grätzel, M. *J. Am. Chem. Soc.* **1993**, *115*, 6382.
(7) O'Regan, B.; Fitzmaurice, D.; Grätzel, M. *Chem. Phys. Lett.* **1991**, *183*, 89.
(8) O'Regan, B.; Fitzmaurice, D.; Grätzel, M. *J. Phys. Chem.* **1991**, *95*, 10525.
(9) Rothenberger, G.; Fitzmaurice, D.; Grätzel, M. *J. Phys. Chem.* **1992**, *96*, 5983.
(10) Redmond, G.; Fitzmaurice, D. *J. Phys. Chem.* **1993**, *97*, 1426.
(11) Redmond, G.; Grätzel, M.; Fitzmaurice, D. *J. Phys. Chem.* **1993**, *97*, 6951.
(12) Fitzmaurice, D. *Sol. Energy Mater. Sol. Cells* **1994**, *32*, 289.
(13) Enright, B.; Redmond, G.; Fitzmaurice, D. *J. Phys. Chem.* **1994**, *98*, 6195.
(14) Flood, R.; Enright, B.; Allen, M.; Barry, S.; Dalton, A.; Doyle, H.; Fitzmaurice, D. *Sol. Energy Mater. Sol. Cells* **1995**, *39*, 83.
(15) Enright, B.; Fitzmaurice, D. *J. Phys. Chem.* **1996**, *100*, 1027.
(16) Lyon, L.; Hupp, J. *J. Phys. Chem.* **1995**, *99*, 15718.
(17) Lemon, B.; Hupp, J. *J. Phys. Chem.* **1996**, *100*, 14578.
(18) Zaban, A.; Meier, A.; Gregg, B. *J. Phys. Chem. B* **1997**, *101*, 7985.
(19) Cao, F.; Oskam, G.; Searson, P.; Siripala, J.; Heimer, T.; Farzad, F.; Meyer, G. *J. Phys. Chem.* **1995**, *99*, 11974.
(20) Kay, A.; Humphry-Baker, R.; Grätzel, M. *J. Phys. Chem.* **1994**, *98*, 8. 952.
(21) Boschloo, G.; Goossens, A.; Schoonman, J. *J. Electroanal. Chem.* **1997**, *428*, 25.
(22) Kavan, L.; Kratochvilov, K.; Grätzel, M. *J. Electroanal. Chem.* **1995**, *394*, 93.
(23) Kavan, L.; Grätzel, M.; Rathousky, J.; Zucal, A. *J. Electrochem. Soc.* **1996**, *143*, 394.
(24) Södergren, S.; Siegbahn, H.; Rensmo, H.; Lindström, H.; Hagfeldt, A.; Lindquist, S.-E. *J. Phys. Chem. B* **1997**, *101*, 3087.
(25) Lindström, H.; Södergren, S.; Solbrand, A.; Rensmo, H.; Hjelm, J.; Hagfeldt, A.; Lindquist, S.-E. *J. Phys. Chem. B* **1997**, *101*, 7710.
(26) Lindström, H.; Södergren, S.; Solbrand, A.; Rensmo, H.; Hjelm, J.; Hagfeldt, A.; Lindquist, S.-E. *J. Phys. Chem. B* **1997**, *101*, 7717.
(27) Solbrand, A.; Lindström, H.; Rensmo, H.; Hagfeldt, A.; Lindquist, S.-E.; Södergren, S. *J. Phys. Chem. B* **1997**, *101*, 2514.
(28) Vogel, R.; Hoyer, P.; Weller, H. *J. Phys. Chem.* **1994**, *98*, 3183.
(29) Hotchandani, S.; Kamat, P. V. *J. Electrochem. Soc.* **1992**, *139*, 1630.

(30) Redmond, G.; Burgess, C.; O'Keefe, A.; MacHale, C.; Fitzmaurice, D. *J. Phys. Chem.* **1993**, *97*, 11111.
(31) Hoyer, P.; Eichberger, R.; Weller, H. *Ber. Bunsen-Ges. Phys. Chem.* **1993**, *97*, 630.
(32) Hoyer, P.; Weller, H. *J. Phys. Chem.* **1995**, *99*, 14096.
(33) Rensmo, H.; Keis, K.; Lindström, H.; Södergren, S.; Solbrand, A.; Hagfeldt, A.; Lindquist, S.-E.; Wang, L.; Muhammed, M. *J. Phys. Chem. B* **1997**, *101*, 2598.
(34) Lemon, B.; Hupp, J. *J. Phys. Chem. B* **1997**, *101*, 2426.
(35) Bedja, I.; Hotchandani, S.; Kamat, P. V. *J. Phys. Chem.* **1994**, *98*, 4133.
(36) Kamat, P. V.; Bedja, I.; Hotchandani, S.; Patterson, L. *J. Phys. Chem.* **1996**, *100*, 4900.
(37) Björkstén, U.; Moser, J.; Grätzel, M. *Chem. Mater.* **1994**, *6*, 858.
(38) Hotchandani, S.; Bedja, I.; Fessenden, R.; Kamat, P. V. *Langmuir* **1994**, *10*, 17.
(39) Finklea, H. *Semiconductor Electrodes*; Studies in Physical and Theoretical Chemistry 55; Elsevier Science: Amsterdam, 1988.
(40) Morrison, S. *Electrochemistry at Semiconductor and Oxidised Metal Electrodes*; Plenum Press: New York, 1980.
(41) Liu, C. Y.; Bard, A. *J. Phys. Chem.* **1989**, *93*, 7749.
(42) Burstein, E. *Phys. Rev.* **1952**, *93*, 632.
(43) Pankove, J. *Optical Processes in Semiconductors*; Dover Publications: New York, 1971.
(44) Tomkiewicz, M. *J. Electrochem. Soc.* **1979**, *126*, 1505.
(45) Grätzel, M. *Heterogeneous Photoelectrochemical Electron Transfer*; CRC Press: Boca Raton, 1989, p 115.
(46) Siripala, W.; Tomkiewicz, M. *J. Electrochem. Soc.* **1982**, *129*, 1240.
(47) Miki, T.; Yanagi, H. *Langmuir* **1998**, *14*, 3450.
(48) Lunell, S.; Stashans, A.; Ojamäe, L.; Lindström, H.; Hagfeldt, A. *J. Am. Chem. Soc.* **1997**, *119*, 7374.
(49) Boschloo, G.; Fitzmaurice, D. Manuscript in preparation.